© Universiti Tun Hussein Onn Malaysia Publisher's Office

IJIE

http://penerbit.uthm.edu.my/ojs/index.php/ijie
ISSN : 2229-838X e-ISSN : 2600-7916

The International Journal of Integrated Engineering

A Numerical Model for Analysis of Heat Transfer in MHD Casson Fluid with Radiation and Viscous Dissipation

Gollapalli Shankar[1], Siva Reddy Sheri[1*]

[1]Department of Mathematics,
GITAM School of Science, Sangareddy District, 502329, TELANGANA

*Corresponding author

DOI: https://doi.org/10.30880/ijie.2023.25.05.016
Received 20 January 2023; Accepted 19 June 2023; Available online 19 October 2023

Abstract: This article is, concerned a numerical model for analysis of heat transfer (HT) in MHD Casson fluid including radiation and viscous dissipation. The governing PDE's are derived for the physical model and transformed into non-dimensional form and then using Galerkin finite element method (GFEM) solution is obtained. The impact of dimensionless parameters which are controlling the flow such as thermal Grashof number(Gr), Casson parameter (α) Magnetic parameter (M), Permeability of porous medium (K), Prandtl number (Pr), Heat absorption parameter (Q), Viscous dissipation (Ec) and Radiation parameter (R) are analyzed through graphs for fluid properties. The present results are compared with earlier reported studies for correctness.

Keywords: Heat transfer, MHD, Casson Fluid (CF), radiation, viscous dissipation, GFEM

1. Introduction

Casson Fluid (CF) flow is the most significant fluid because of its sky-high viscosity and low-set shear rate. Among non-Newtonian fluids, the vast range of Casson fluid flow presentations in manufacturing processes, medicinal yields, fake oils, food-processing, gelatine, synovial liquids, blood models, etc. has attracted significant scientific attention. Particularly for a flow via tiny blood capillaries, the Casson fluid flow more fully reveals the blood flow dynamics at low shave responsibilities. Recent developments in MHD Casson fluid flow have drawn researchers' attention to a wide range of industrial technology applications, some of which are the distribution of biochemical unused controller, the treatment of atomic surplus, and the structure of MHD influence producers. Casson [1] introduced Casson fluid initially and cited its significant practical applications. Mustafa et al. [2] lectured irregular HT flow of a Casson liquid through an analogous free stream in a rotating plate. Mukhopadhyay et al. [3] inspected the exact solution of MHD Casson liquid flow toward a linearly stretching surface with transpiration. Many researchers [4-6] have been inspected the MHD Casson liquid with thermal and heat generation through a plate. Shah, et al. [7] calculated the effect of of hall current with thermal radiation on MHD Casson liquid. More recently, Krishna [8] scrutinized the flow of CFF with slip.

Additionally, thermal radiation HT is becoming more and more important in a wide range of engineering research, including compound materials, automation, solar control, aircraft, and extra complicated operational schemes. Furthermore, high HT happens throughout several technical activities. A relatively homogeneous reaction occurs continuously, regardless of the stage, in contrast to the heterogeneous reactions, which only happen within a small radius. A highly homogeneous chemical reaction has a wide range of technical applications, including the oxidation of solid materials, the generation of polymers, drying and dehydration processes, the synthesis of ceramic materials, the manufacture of pottery and glassware, and food processing facilities. Bestman and Adjepong [9] inspected the radiative heat transfer on buoyancy induced power-law fluid over a plate. Gebhart [10] thought carefully on the plate's steady and viscous heat flow. The detailed applications and heat and mass transfer were studied by the authors [11-15]. Eckert [16], illustrated analysis of transfer (heat & mass). Brewster [17] explored the properties of Thermal Radiative

*Corresponding author: sreddy7@yahoo.co.in

Transfer. A sheet containing convective BCs was seen to have stagnation-point flow, according to Hayat et al. [18]. The researchers [19-21], studied the nature of various parameters with Casson liquid. Recently Khalid et al. [22,23] studied MHD Casson fluid with wall temperature.

In the present work, which is driven by the aforementioned discoveries, the heat transport in MHD casson fluid with radiation and viscous dissipation is the major emphasis. A mathematical model's governing equations are created, then transformed into a few PDEs and solved using GFEM. The impact of main physical parameters which are controlling the flow are examined and discussed via plots on velocity and temperature profiles. For this analysis, comparisons are made with formerly published work in the1absence of few parameters and results are found to be in a superior agreement.

2. Mathematical Formulation

Consider the transient MHD boundary layer flow of an incompressible CF flow of a oscillating vertical plate with varying temperature affected by uniform moving magnetic field. A standardized uniform magnetic field B_0 is implemented in a direction parallel y' to -axis. The coordinate system is selected in such a way that x'-axis is upward to the plate and y'--axis is perpendicular (normal) to the plate. Also radiation and viscous dissipation is taken into account. Further, the plate and fluid initially rest for the period $t' < 0$and are held a uniform temperature (UT) T'_∞. At any point inside the fluid $y' \geq 0$, and on the surface of the plate will be preserved uniformly. The fluid temperature of the plate are inverted to a UT T'_∞, and consequently retained.

The following assumptions are made: (i) Due to low Reynolds number, induced magnetic field is not taken within consideration; (ii) In the equation of energy, viscosity dissipation is ignored; (iii) In Boussinesque's approximation, the effects of density fluctuations and mass concentration are taken into account; (iv) In the process of a non-scattering average, a thin liquid is considered to be both emitting and absorbing radiation; and (v) All liquid the terms included in the Casson fluid flow constitutive equation. The physical representation of the issue is shown in Fig.1.

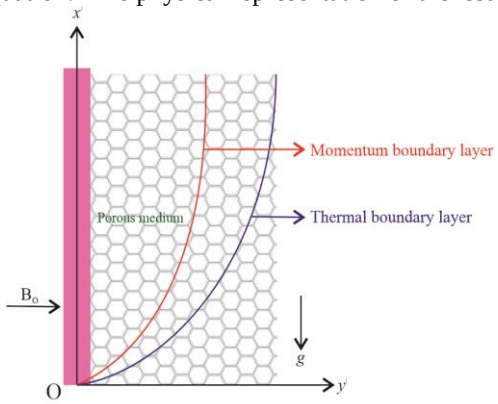

Fig. 1 – Physical model and coordinate system

The initial moment,$t' = 0$, is supposed to be one in which the fluid and plate are both at rest and at a constant temperature, t'. The plane of plate starts oscillating in its plane at time $t' = 0^+, (y' = 0)$ as shown by:

$$V = UH(t)cos(\omega' t')i \; ; or \; V = Usin(\omega' t')i \; ; \;\; t > 0, \tag{1}$$

$$\tau_{ij} = \begin{Bmatrix} 2\left(\mu_B + \frac{P_y}{\sqrt{2\pi}}\right)e_{ij}, \pi > \pi_c \\ 2\left(\mu_B + \frac{P_y}{\sqrt{2\pi_c}}\right)e_{ij}, \pi < \pi_c \end{Bmatrix} \tag{2}$$

The conditions that govern the flow equations are as follows:

$$\frac{\partial u'}{\partial y'} = 0 \tag{3}$$

$$\frac{\partial u'}{\partial t'} = \nu\left(1 + \frac{1}{\alpha}\right)\frac{\partial^2 u'}{\partial y'^2} - \frac{\sigma B_0^2}{\rho}u' - \frac{\nu\phi}{k}u' + g\beta_T(T' - T'_\infty) \tag{4}$$

$$\frac{\partial T'}{\partial t'} = \frac{k}{\rho c_p}\frac{\partial^2 T'}{\partial y'^2} + \frac{\nu}{c_p}\left(\frac{\partial u'}{\partial y'}\right)^2 - \frac{1}{\rho c_p}\frac{\partial q'_r}{\partial y'} - \frac{Q_0}{\rho c_p}(T' - T'_\infty) \tag{5}$$

With the limitations:

$$\begin{gathered} t' \le 0;\ u' = 0\ ;\ T' = T'_\infty \quad for\ y' \ge 0 \\ t' > 0;\ u' = U\,\mathrm{H}(t)\cos(\omega' t')\ or\ u' = U\sin(\omega' t'),\ T' = T'_W \ \ at\ \ y' = 0 \\ u' \to 0\,, T' \to T'_\infty\ \ as\ \ y' \to \infty \end{gathered} \tag{6}$$

Rosseland estimate is:

$$\mathrm{q_r}' = -\frac{4\sigma^*}{3\mathrm{k}^*}\frac{\partial \mathrm{T}'^4}{\partial \mathrm{y}'} \tag{7}$$

$$\mathrm{T}'^4 \cong 4\mathrm{T}'^3_\infty \mathrm{T}' - 3\mathrm{T}'^4_\infty \tag{8}$$

using Eqs (7) & (8) in Eq (5) gives the following PDE:

$$\frac{\partial T'}{\partial t'} = \frac{k}{\rho c_p}\frac{\partial^2 T'}{\partial y'^2} + \frac{v}{c_p}\left(\frac{\partial u'}{\partial y'}\right)^2 + \frac{1}{\rho c_p}\frac{16\sigma^* T'^3_\infty}{3k^*}\frac{\partial^2 T'}{\partial y'^2} - \frac{Q_0}{\rho c_p}(T' - T'_\infty) \tag{9}$$

Succeeding Non-dimensional variables and parameters are familiarized:

$$\begin{gathered} u = \frac{u'}{U}\,, y = \frac{y'U}{v}\,, t = \frac{U^2 t'}{v}\,, M = \frac{\sigma B_0^2 v}{\rho U^2}\,, \frac{1}{K} = \frac{\varphi v^2}{k_1 U^2}, Gr = \frac{g\beta_T (T'_w - T'_\infty)v}{U^3}, \\ R = \frac{4\sigma^* T'^3_\infty}{kk^*}\,, Pr = \frac{\rho v C_p}{k}\,, Q = \frac{vQ_0}{\rho c_p U^2}, Ec = \frac{U^2}{c_p (T'_w - T'_\infty)}\,, \theta = \frac{T' - T'_\infty}{T'_w - T'_\infty}\,, \omega = \omega'\frac{v}{U^2} \end{gathered} \tag{10}$$

From above, we get the resultants PDE's are:

$$\frac{\partial u}{\partial t} = \left(1 + \frac{1}{\alpha}\right)\frac{\partial^2 u}{\partial y^2} - Mu - \frac{1}{K}u + Gr\theta \tag{11}$$

$$\frac{\partial \theta}{\partial t} = \left(1 + \frac{4R}{3}\right)\frac{1}{Pr}\frac{\partial^2 \theta}{\partial y^2} + Ec\left(\frac{\partial u}{\partial y}\right)^2 - Q\theta \tag{12}$$

The transformed BCs are:

$$\begin{gathered} t \le 0;\ u = 0, \theta = 0\ \ for\ all\ \ y > 0 \\ t \ge 0\ ;\ u = H(t)\ \cos(\omega t)\ \ or\ \ u = sin(\omega t),\ \ \theta = 1\ \ at\ \ y = 0, \\ u \to 0,\ \theta \to 0,\quad as\ \ y \to \infty \end{gathered} \tag{13}$$

The skin friction (τ)& Nusselt number (Nu) is specified by:

$$\tau = -\left(1 + \frac{1}{\gamma}\right)\left(\frac{du}{dy}\right)_{y=0} \tag{14}$$

$$Nu = -\left(\frac{d\theta}{dy}\right)_{y=0} \tag{15}$$

3. Method of Solution

The Non-dimension PDE's [11] & [12] are solved along the BC's [13] by using GFEM (Bathe [24], Reddy [25], Connor and Brebbia [26] and Chung [27]) and their solutions are presented. The basic steps concerned are as in Figure 1.

4. Validation of the Code

To test the effectiveness of the current findings, a quantitative study of the pertinent (available) literature was carried out in the absence of the dimensionless values $M = 0, K = 0, R = 0, Ec = 0\ and\ Q = 0$, and it was found to be an exact match with Khalid et al. [22] and [23]. In Table 1-3, the computational estimates for the skin factor and Nusselt number are shown to be in outstanding agreement with the outcomes of published investigations.

5. Results and Discussion

For knowing the physics behind the mathematical model, a numerical study has been conducted and outcomes are discussed via plots. The differences in the most important regulating factors like (α), (Q),(M),(K),(Ec),(R),(Pr), in Figs 2-15 affect the fluid characteristics like speed, temperature, skin friction, and Nusselt number of fluid. In the current investigation, we presumptively used the following values for the finite element calculations non-attendance parameters $\mathrm{Gr} = 2.0,\ \alpha = 1.0,\ \mathrm{M} = 1.0,\ \mathrm{K} = 1.0,\ \mathrm{Pr} = 0.71,\ \mathrm{R} = 1.0,\ \ \mathrm{Ec} = 0.1,\ \mathrm{Q} = 1.0, \mathrm{t} = 1.0,\ \omega\mathrm{t} = 0.$ Otherwise the values are indicated in figures and tables. The effect of the thermal Grashof number on velocity is depicted in Fig. 2. The thermal Grashof number identifies the interaction between the thermal buoyancy force and the viscous hydrodynamic force in the boundary layer. It is evident that the velocity rises as the thermal buoyancy force rises, as expected. Positive Gr values in this instance signify cooling of the plate. Additionally, when Gr increases, the peak values of the velocity increase rapidly towards the porous plate before steadily dropping to the free stream velocity. The graphical representation of M in Fig. 3 emphasizes the fluid's velocity. The fluid velocity decreases as the magnetic field's intensity rises, as can be seen.

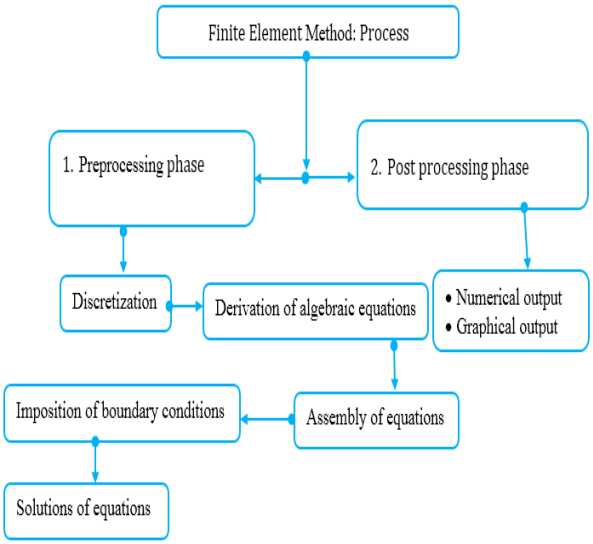

Fig. 1 - Fundamental steps of finite element modelling

Table 1 - Outcome of *Pr*, *Gr*, *α*, *ωt*, *M*, *K* and *t* on *τ* with *R* = 0, *Ec* = 0and *Q* = 0

Pr	Gr	α	ωt	M	K	t	Previous results [22] τ	Present results τ
0.3	3.0	0.5	0.25π	0.5	0.2	0.3	1.02992	1.029925712
0.71	3.0	0.5	0.25π	0.5	0.2	0.3	1.29166	1.291665815
0.3	5.0	0.5	0.25π	0.5	0.2	0.3	0.856995	0.856995728
0.3	3.0	1.0	0.25π	0.5	0.2	0.3	0.93952	0.939526532
0.3	3.0	0.5	0.25π	0.5	0.2	0.3	1.05009	1.050099722
0.3	3.0	0.5	0.25π	1.0	0.2	0.3	1.08472	1.084728515
0.3	3.0	0.5	0.25π	0.5	1.0	0.3	0.670207	0.670207592
0.3	3.0	0.5	0.25π	0.5	0.2	0.5	0.692367	0.692367285

Table 2 - Effect of *Pr*, *Gr*, *α*, *ωt* and *t* on *τ* with *M* = 0, *K* = 0, *R* = 0, *Ec* = 0 and *Q* = 0

Pr	Gr	α	ωt	t	Previous results [22] τ	Present results τ
0.3	3.0	0.5	0.25π	0.3	3.384043	3.384042653
0.71	3.0	0.5	0.25π	0.3	0.437932	0.437931962
0.3	5.0	0.5	0.25π	0.3	0.200932	0.200932016
0.3	3.0	1.0	0.25π	0.3	0.536355	0.536354982
0.3	3.0	0.5	0.25π	0.3	0.422417	0.422416891
0.3	3.0	0.5	0.25π	0.4	0.307634	0.307633796

The velocity is slowed down by the obstruction (Lorentz) force, which is caused by greater values of M in the direction of the fluid flow that is opposing the flow, as shown in the image. On the speed profiles, Fig. 4 considers different quantities of the permeability parameter *K*. Evidently, if *K* concentrations increase, the permeable walls'

velocities will likely increase as well, which will increase the thickness of the momentum limit layer. The speed of the liquid was seen inside the vertical surfaces that it employed below the permeability that was less important. As the Casson fluid flow (CFF) parameter is increased, as illustrated in Fig. 5, the velocity decreases. The physics is that by lowering the yield stress, the velocity boundary is suppressed. A thin boundary layer is produced by the flexibility of the Casson fluid flow, which lowers velocity (u).

Table 3 - Effect of *Pr* and *t* on *Nu* with *M* = 0, *K* = 0, *R* = 0, *Ec* = 0 and *Q* = 0

Pr	*t*	Previous Results [22 & 23] *Nu*	Present results, *Nu*
0.3	0.3	0.564	0.564157
0.71	0.3	0.867	0.867316
0.3	0.6	0.398	0.398279

The yield stress that drives the velocity is subtracted by the CFF parameter, according to the underlying mechanics. Figs. 6 and 7 illustrate the velocity and temperature profiles for different values of the Prandtl number *Pr*. The Prandtl number defines the ratio of momentum diffusivity to thermal diffusivity. The numerical results show that the effect of increasing values of Prandtl number results in a decreasing velocity (Fig. 6). From Fig. 7, it is observed that an increase in the Prandtl number results in a decrease of the thermal boundary layer thickness and in general lower average temperature within the boundary layer. The reason is that smaller values of *Pr* are equivalent to increasing thermal conductivities, and therefore heat can diffuse away from the heated plate more rapidly than for higher values of *Pr*. Hence in the case of smaller Prandtl numbers the boundary layer is thicker, and the rate of heat transfer is reduced. Fig. 8 illustrates how fluctuations in velocity may be used to show how radiation affects velocity. Near the porous plate, it is seen that velocity fields rapidly fall and then gradually increase to their free stream value, which improves the radiation parameter. For various radiation parameter values, the temperature curve is shown in Fig. 9. With an increase in radiation parameter, the temperature profile rises.

For the heat transfer at absorption (Q > 0), Figs. 10 and 11 illustrate the effects of various current levels on fluid velocity and temperature. It is observed that the fluid heat and speed curves diminish as the Q values increase. The fluid temperature in the plate zone is raised because of the energy level being raised by the presence of a temperature difference within the boundary layer, which is the underlying cause of this. Once more, heat flow absorption inside a fluid flow has the opposite effect and reduces the fluid heat. The temperature decreases with an increase in the heat source parameter Q because, when heat is absorbed, the buoyancy force lowers the temperature profiles. This is because buoyancy force decreases and flow rate is delayed when heat is absorbed, which causes a decrease in velocity profiles.

For the heat transfer at absorption (Q > 0), Figs. 10 and 11 illustrate the effects of various current levels on fluid velocity and temperature. It is observed that the fluid heat and speed curves diminish as the Q values increase. The fluid temperature in the plate zone is raised because of the energy level being raised by the presence of a temperature difference within the boundary layer, which is the underlying cause of this. Once more, heat flow absorption inside a fluid flow has the opposite effect and reduces the fluid heat. The temperature decreases with an increase in the heat source parameter Q because, when heat is absorbed, the buoyancy force lowers the temperature profiles. This is because buoyancy force decreases and flow rate is delayed when heat is absorbed, which causes a decrease in velocity profiles.

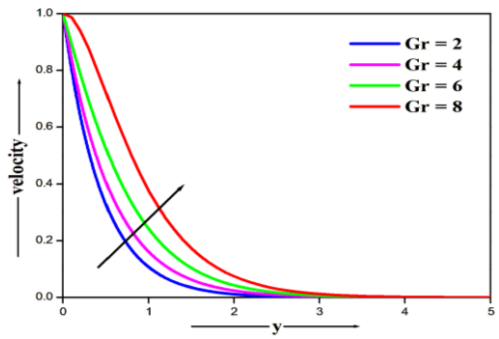

Fig. 2 - Profile of velocity for different values of Gr

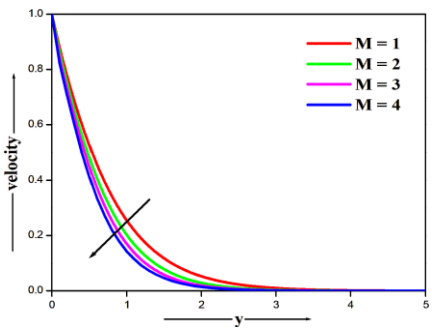

Fig. 3 - Profile of velocity for different values of M

Fig. 12 illustrates the characteristics of u for flow parameters t. It is demonstrated using the field u how the characteristics of velocity vary when t is elevated. Because t expands more readily than the buoyant force, the liquid's speed increases as a result. The manipulate of the Eckert number Ec on boundary layer of velocity, and mass temperature profiles is illustrated in Figs. 13 and 14. Ec Expresses the correlation involving the kinetic energy & enthalpy. Velocity and temperatures are enlarged with rising of Ec. Fig. 15 depicts the velocity distribution caused by

changes in the phase angle ωt . According to the inference, fluid velocity asymptotically tends to zero away from the plate and oscillates between -1 and 1 for any values of phase angle ωt . Thus, we may say that the sinusoidal boundary condition causes the velocity to exhibit an oscillating behavior.

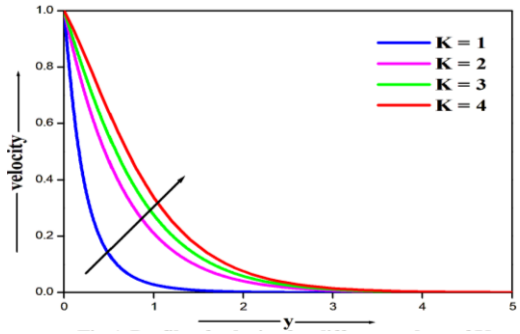

Fig. 4 - Profile of velocity for different values of K

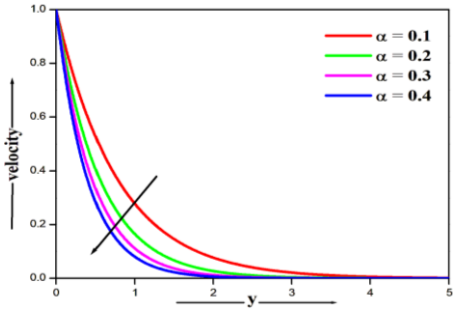

Fig. 5 - Profile of velocity for different values of α

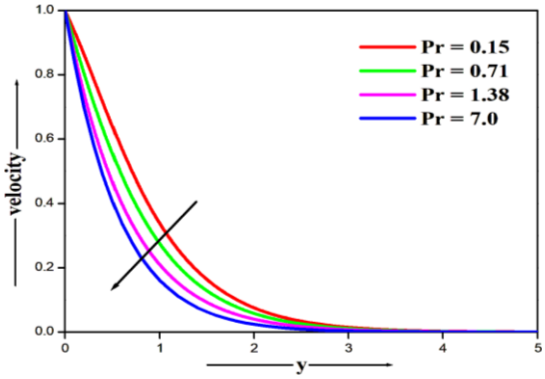

Fig. 6 - Profile of velocity for different values of Pr

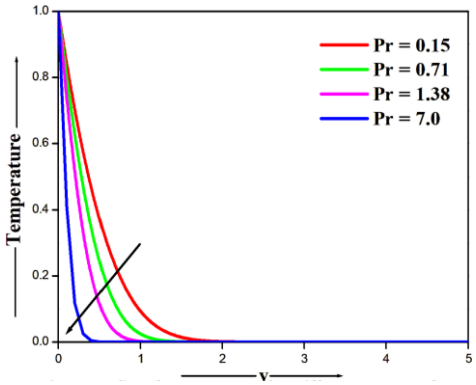

Fig. 7 - Profile of Temperature for different values of Pr

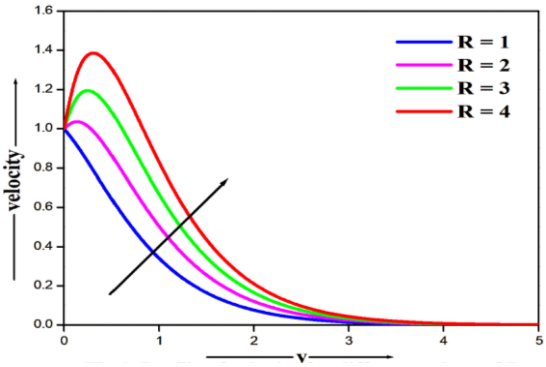

Fig. 8 - Profile of velocity for different values of

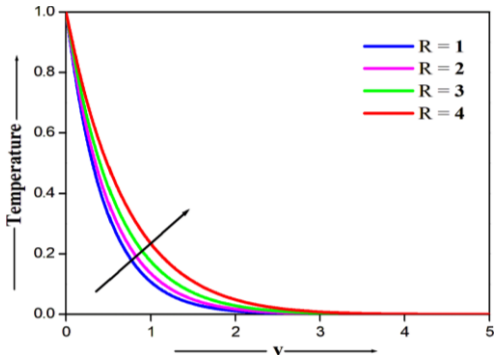

Fig. 9 - Profile of Temperature for different values of R

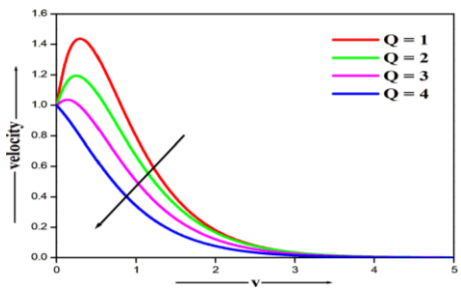

Fig. 10 - Profile of velocity for different values of Q

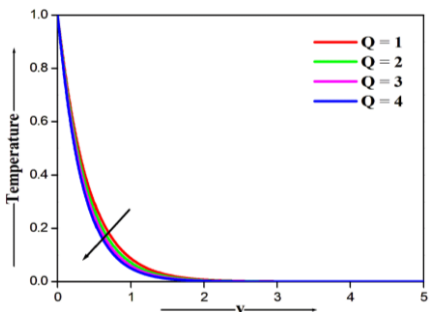

Fig. 11 - Profile of Temperature for different values of Q

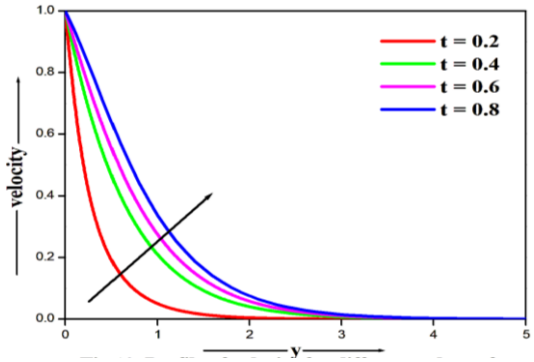

Fig. 12 - Profile of velocity for different values of t

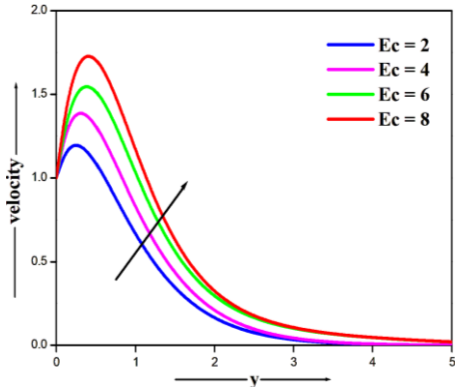

Fig. 13 - Profile of velocity for different values of Ec

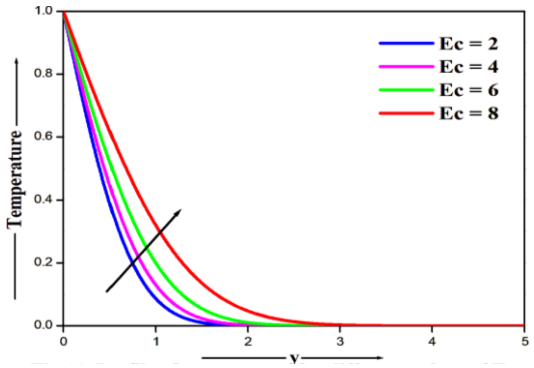

Fig. 14 - Profile of Temperature for different values of Ec

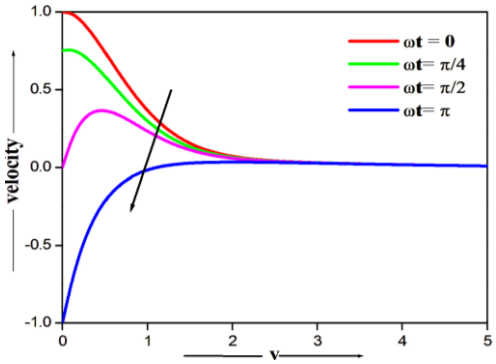

Fig. 15 - Profile of velocity for different values of ωt

6. Conclusions

In this study on a linearly oscillating vertical plate, examining the impact of free convection, viscid dissipation, and radiation flow via a porous Casson fluid medium is of great interest. The effects of changing temperature and velocity are also considered on infinite vertical plate, linearly porous surface. The MATLAB software was used to compare the results using both graphical and numerical solutions. The outcomes of the chosen methodology are consistent with earlier research. The results illustrate the flow characteristics for the velocity, temperature, skin-friction and Nusselt number. As the Casson parameter drops, the layer's velocity profile increases. It happens because of the favourable inertial forces within the porous matrix. As the Prandtl number Pr and the heat source Q parameter grow, the mass temperature distribution decreases in the free convection flow. Boundary velocity profile rises in the presence of Gr, K, R, and Ec. Skin friction and Nusselt number shown in tables 1, 2, and 3 demonstrate that results are in excellent agreement with those obtained by Khalid et al. [22] and [23].

Acknowledgements

Gollapalli Shankarsincerely acknowledges support of Corresponding author and support by Department of Math's, GITAM University, Hyderabad, India.

References

[1] Casson, N. (1959). "A flow equation for the pigment oil suspensions of the printing ink type in Rheology of Disperse Systems". Mill, C.C., Education Pergamon Press, London UK, 84–102.

[2] Mustafa, M., Hayat, T., Pop, I., & Aziz, A. (2011). "Unsteady Boundary Layer Flow of a Casson Fluid Due to an Impulsively Started Moving Flat Plate". *Heat Transfer-Asian Results*, 40, 563-576.

[3] Mukhopadhyay, S., Bhattacharyya, K., & Hayat, T. (2003). "Exact solutions for the flow of Casson fluid over a stretching surface with transpiration and heat transfer effects". *Chinese Physics* B, 22(11) ,114701.

[4] Qasim, M., & Noreen, S. (2004). "Heat transfer in the boundary layer flow of a Casson fluid over a permeable shrinking sheet with viscous dissipation". *The European Physics Journal Plus*, 129.

[5] Hussanan, A., Zuki Salleh, M., Tahar, R.M., & Khan, I. (2014). "Unsteady Boundary Layer Flow and Heat Transfer of a casson Fluid past an Oscillating Vertical Plate with Newtonian Heating". *PLoS* ONE, 9(10), e108763.
[6] Hussanan, A., Salleh, M.Z., Khan, I., & Tahar, R.M. (2016). "Unsteady heat transfer flow of a casson fluid with Newtonian heating and thermal radiation". *Journal Teknologi*, 78, 4-4.
[7] Shah, Z., Islam, S., Ayaz, H., & Khan, S. (2019). "Radiative heat and mass transfer analysis of micro polar Nano fluid flow of casson fluid between two rotating parallel plates with effects of hall current". *ASME Journal of Heat Transfer*, 141(2), 022401.
[8] Krishna, M.M. (2020). "Numerical investigation on magneto hydrodynamics flow of Casson fluid over a deformable porous layer with slip". *Indian Journal of Physics*, 94(12), 2023-2032.
[9] Bestman, A.R., &Adjepong, S.K. (1988). "Unsteady hydromagnetic free-convection flow with radiative heat transfers in a rotating fluid". *Astrophysics and Space Science*, 143, 73-80.
[10] Gebhar, B. (1962). "Effects of viscous dissipation in natural convection". *Journal of Fluid Mechanics*, 14(2), 225–232.
[11] Sundalgekar, V.M. (1972). "Viscous dissipation effects on unsteady free convective flow past an infinite vertical porous plate with constant suction". *International Journal of Heat and Mass Transfer*, 15, 1253-1261.
[12] Israel-Cookey, C., Ogulu, A., &Omubo-Pepple, V.B. (2003). "Influence of Viscous Dissipation and Radiation on Unsteady MHD Free-Convection Flow past an Infinite Heated Vertical Plate in a Porous Medium with Time-Dependent Suction". *International Journal of Heat and Mass Transfer*, 46, 2305-2311.
[13] Hasimoto, H. (1957). "Boundary layer growth on a flat plate with suction or injection". *Journal of the Physical Society of Japan*, 12(1), 68-72.
[14] Yamamoto, K., &Iwamura, N., (1976). "Flow with convective acceleration through a porous medium". *Journal of Engineering Mathematics*,10, 41-54.
[15] Mansutti, D., Pontrelli, G., & Rajagopal. K.R. (1993). "Steady flows of non-Newtonian fluids past a porous plate with suction or injection". *International Journal of Numerical Methods of Fluids*, 17, 927-941.
[16] Eckert, E.R.G., & Drake, R.M. (1972). "Analysis of heat and mass transfer": *Mac-Graw Hill Book company Network*.
[17] Brewster, M.Q. (1972). "Thermal Radiative Transfer Properties New York": Wiley.
[18] Hayat, T., Shehzad, S.A., Alsaedi, A., &Alhothuali, M.S. (2012). "Mixed convection stagnation point flow of Casson fluid with convective boundary conditions". *Chinese Physics Letters*, 29 (11), 114704.
[19] Mukhopadhyay, S., (2013). "Effects of thermal radiation on Casson fluid flow and heat transfer over an unsteady stretching surface subjected to suction/blowing". *Chinese Physics B*, 22 (11), 114702.
[20] Bhattacharya, K. (2013). "Boundary layer stagnation-point flow of casson fluid and heat transfer towards a shrinking/strectching sheet". *Frontiers Heat Mass Transfer*, 4(2) ,023003.
[21] Mukhopadhyay, S., De Rajan P., &Bhattachayya, K. (2013). "Casson fluid flow over an unsteady stretching surface". *Ain Shams Engineering Journal*, 4, 933-938.
[22] Asma Khalid, Ilyas Khan, Arshad Khan, &SharidanShafie. (2015). "Unsteady MHD free convection flow of Casson fluid past over an oscillating vertical plate embedded in a porous medium". *Engineering Science and Technology an International Journal*, 18, 309-317.
[23] Asma Khalid, Ilyas Khan, SharidanShafie, (2015a). "Exact solutions for unsteady free convection flow of casson fluid over an oscillating vertical plate with constant wall temperature". *Abstract and Applied Analysis*, 8, 946350.
[24] Bathe, K.J. (1996). "Finite Element Procedures New Jersey USA": Prentice-Hall
[25] Reddy, J.N. (1985). "An Introduction to the Finite Element Method New York": McGraw-Hill,
[26] Connor, J.J., &Brebbia, C.A. (1976). "Finite Element Techniques for Fluid Flow Butter worth's London".
[27] Chung, T.J. (1978). "Finite element analysis in fluid dynamics. Research supported by the U.S. Air orce and U.S. Army New York": McGraw Hill International Book Co. 389.